Hydrogeochemical study concerning fluoride appraisal in groundwater - A case study from a tropical region of Central India

Jagriti Khichariya, Yashu Baghel✉
jagriti.khichariya@bitdurg.ac.in[1], dr_yashu_verma@yahoo.com[2]
Bhilai Institute of Technology, Durg, 491001,C.G., India
Corresponding author:- dr_yashu_verma@yahoo.com
(Orcid id- 0000000336985262)

Abstract

A total of 32 groundwater samples collected from two blocks in the Gariyaband District of Chhattisgarh, India, were analyzed to investigate the spatial and temporal variability of fluoride contamination. Precise fluoride concentration in the groundwater was measured using a fluoride ion-selective electrode. The Piper trilinear diagram and Gibbs plot were generated using MODFLOW and PHREEQC models to study factors controlling groundwater chemistry. Groundwater samples from both the blocks revealed a maximum of 4.0 mg/L fluoride in the pre-monsoon season (PRMS) and 6.2 mg/L fluoride during the post-monsoon season (POMS), which are beyond the permissible limits specified by the WHO and BIS (1.5 mg/L) in drinking water. The statistical analysis revealed that a high third quartile score (Q3) for Cl^- and max. score for Ca^{2+} (Box-Whisker plot) in Devbhog relate to higher F^- concentrations in groundwater. Statistical analysis showed the general dominance of the cations $Na^+ > Ca^{2+} > Mg^{2+} > K^+$ and the anions $Cl^- > HCO_3^- > SO_4^{2-} > F^-$ in the groundwater. Pearson correlation analysis presented a low positive correlation of F^- with Na^+ ($r<0.1$); $p<0.001$ during PRMS, and a significantly strong correlation with Ca^{2+} and CO_3^{2-} ($r>0.6$); $p<0.001$ during the POMS. The region is dominated by Ca- Mg-Cl-HCO_3 type water. Characterization of the rocks using SEM-EDX confirmed the presence of fluoride-rich minerals, whose weathering and subsequent dissolution as the primary factors influencing ionic chemistry in groundwater.

Keywords: Hydro-chemistry, fluoride, box plot, Pearson correlation, chloroalkaline indices

1. INTRODUCTION

The quality of groundwater is a critical issue when it comes to its safety for drinking. Several factors influence groundwater quality, including dissolution and precipitation, surface runoff,

groundwater movement, catchment area features, pumping activities, residence period and soluble content of the minerals (De Giglio et al., 2015; NGWA,1999). Naturally, when water moves slowly through the rocks and sediments of the Earth's crust, it reacts with minerals and gases, changing its chemical composition (Elango & Kannan, 2007). Groundwater extraction results in massive weathering of rocks, leading to the release and transport of contaminants in the aqueous phase. India has 18% of the world's population, but only 4% of its water resources make it among the most water-stressed regions in the world (Briscoe & Malik, 2005). Aquifers have supplied a significant portion of the country's rising water demand in recent years, and groundwater has slowly become the foundation of India's agricultural and drinking water security (Shankar et al., 2011). Groundwater used for domestic use, accounts for 9% of the extracted groundwater (Reddy et al., 2019). From the total available extractable groundwater resources in Chhattisgarh state, 3.83% are considered critical, while 18.79% are considered semicritical (CGWB, 2023).

When some contaminants exceed the standards set for drinking water, they are referred to as groundwater pollutants (Suhag, 2016). Fluoride dissolution in groundwater has been linked to dental and skeletal fluorosis disease in humans, which is reported in several countries (Podgorski & Berg 2022). The Pacific volcanic belt, the East African Rift Valley, the cratonic regions of central Africa, Asia, and North and South America, the huge sedimentary basins in South America, China, and the desert area along the US-Mexico border are all considered critical zones (Garcia and Borgnino, 2015).

In several regions of India, groundwater contaminated with F^- exceeded the safe permissible limit of 1.5 mg/L as specified by the WHO (Kashyap et al., 2021). Hydrogeochemical processes such as ion-exchange reactions (Laxmankumar et al., 2019), depletion of Ca^{2+} in an alkaline medium (high pH) (Brindha & Elango, 2011), $CaCO_3$ precipitation due to common ion effects (Sivasankar et al., 2016), complexation of Ca^{2+} (Dhiman & Keshari, 2006), and SiO_2 weathering (Khichariya & Verma, 2021) are favorable for the dissolution of fluoride into aqueous media. The weathering of rocks containing fluoride minerals (Chakraborty et al., 2018) and evapotranspiration (Reddy et al., 2016) processes also govern fluoride enrichment in groundwater. The principal minerals hosting fluoride such as apatite, biotite, muscovite, chlorite, sericite, hornblende, and kaolinite, present in the gneissic and granitic rocks of the region are the key geogenic sources of fluoride in the area due to prolonged rock–water interactions (Tiwari et al., 2020).

The geologic source of elemental mobilization from minerals and human activities can significantly contribute to increased concentrations of elements in groundwater sourced from hand pump wells (Sen & Peucker-Ehrenbrink, 2012). The concentrations of elements are minimal in water flowing along unaltered pathways such as surface or groundwater within an aquifer. The interception of water

through pumping wells alters natural flow, which may influence the quality of water withdrawn from wells (Ayotte et al., 2011).

Among 27 districts in Chhattisgarh, nearly 17 have been reported to contain fluoride in drinking water above the permissible limit (1.5 mg/L). Two-hand pumps in the tribal blocks of the Gariyaband district contaminated with fluoride have been closed for drinking purposes since 2015 (The Economic Times, 2015). Groundwater's dynamic qualities make it an effective conduit for contaminants, allowing them to travel significant distances over extended periods under different climatic conditions. Due to the unavailability of sufficient data on fluoride concentration in the groundwater of Gariyaband district after 2015, this work investigates and evaluates the extent of temporal and spatial variations in the fluoride concentration of groundwater samples from two blocks of the Gariyaband district. The hydrogeochemical and mineralogical study of the water and rock samples will elucidate the genesis and mechanism behind fluoride enrichment, helping authorities take mitigative steps for water quality vulnerability in the region.

2. MATERIALS AND METHOD

2.1Study area

The Gariyaband district is geographically located at latitude 20.6348° N and longitude 82.0615° E in the eastern part of Chhattisgarh state of India. Out of five blocks of this district, Mainpur is located at the latitude 20.1332° N, longitude 82.3016° E, covering an area of 6.7 Km^2 and Devbhog is located at the latitude 19.9137° N and longitude 82.6432° E (3.01 Km^2) southwards of Gariyaband district. Mainpur and Devbhog lie in the subbasin of the Telnadi River, which flows from south to north, forming the Orissa state border (Tel, 2008). The topographic features of the district indicate that the district is moderately inclined northward (PMKSY scheme, 2016), i.e., from Devbhog toward Mainpur. The study area experiences tropical climatic conditions with a minimum temperature of 10.2°C in winter and a maximum temperature of 44°C in summer. The average rainfall distribution in the district is 1037.47 mm from southwestern monsoon winds (June–September) (Manjhi, 2019). Rocks from the Eastern ghat and Bengpal group constituting metamorphic and igneous type dominate the southern part of the district (Updated district survey report of Gariyaband 2020).

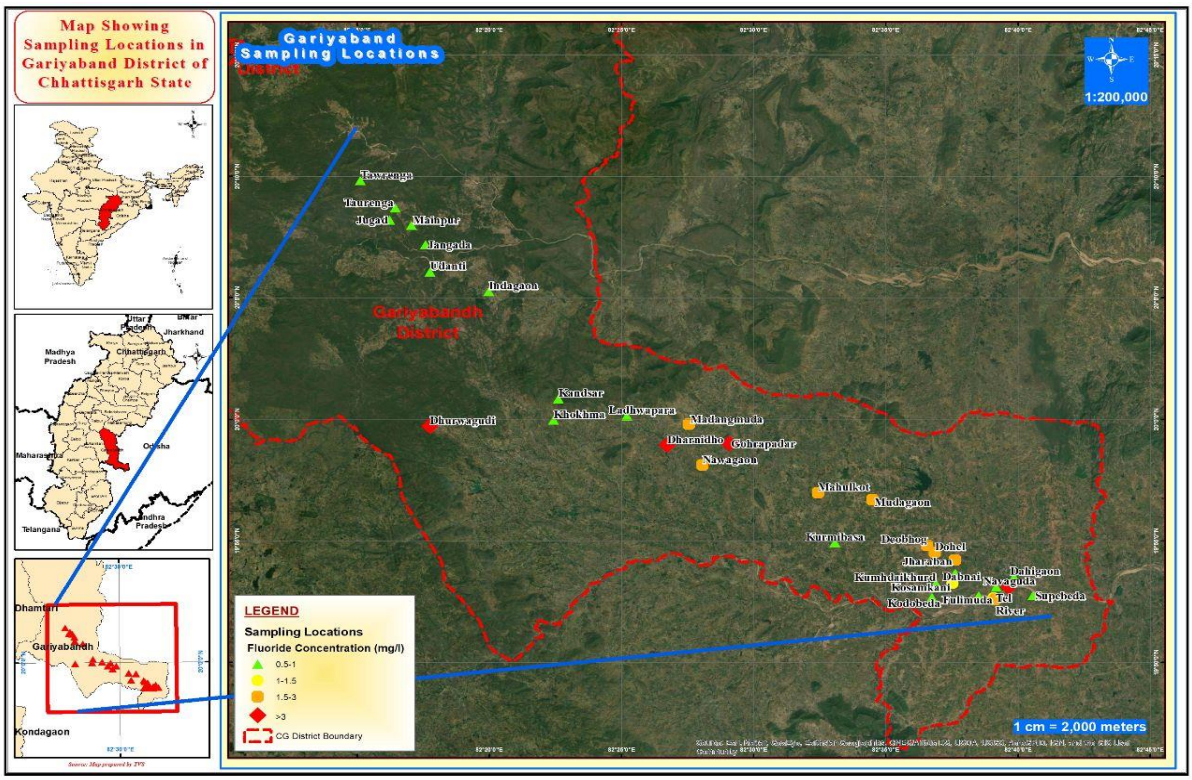

Fig.1. Groundwater sampling locations in Gariyaband District

2.2 Data Collection

Groundwater samples were collected during the post-monsoon season (October 2020) and pre-monsoon season (May 2021) from 32 sampling locations (handpumps) in two blocks (Mainpur and Devbhog) of the Gariyaband district of Chhattisgarh state, covering an area of ≈10 Km^2. The depth of hand pumps from the sampling stations was collected from the Public Health Engineering (PHE) office, in Gariyaband, Chhattisgarh. A geographic information system (ESRI ArcGIS desktop 10.5 version) was used to create location points of handpumps in the map (Fig.1). Sampling locations were chosen along the direction of groundwater flow away from the fluoride-contaminated region in the Devbhog block (6.2 mg/L).

2.3 Quality control and Quality assurance

Duplicate drinking groundwater samples were collected from handpumps after purging 4-5 times in cleaned 1000 mL polyethylene bottles prewashed with deionized water. Properly labeled bottles (location) were kept in a cool box and refrigerated at 4°C in the lab for chemical analysis. Water samples were collected in an acidified bottle (0.05 M HNO_3) for metal analysis.

2.4 Data Analysis

2.4.1 Groundwater samples

A cluster sampling technique was used to collect groundwater samples from both blocks to analyze physio-chemical parameters. The groundwater sampling network was based on the distance from the maximum fluoride contaminant location (Devbhog block) toward the slope of the district to study the extent of plume behavior in groundwater. Physical parameters including temperature, pH, electrical conductivity (EC) oxidation-reduction potential (ORP), dissolved oxygen (D.O.) and total dissolved solids (T.D.S.) were measured in situ by a portable digital electronic water analyzer kit (MAC-551). To ensure the accuracy and reliability of results standard reference 0.1M NaF (Orion), was used to prepare different concentrations of fluoride. Fluoride levels in the water samples were measured in situ using a benchtop ion-selective meter with an electrode (Thermo Scientific Orion Star A214), operating at a range of 0.0001 to 19900 mg/L and interferences of ions were eliminated using TISAB III. Chemical analysis of the groundwater was performed according to the Standard Methods for Examination of Water and Wastewater (APHA, 2017). The acid titration determined the hydroxide (OH^-), carbonate (CO_3^{2-}) and bicarbonate (HCO_3^-) alkalinity and argentometric titration determined chloride (Cl^-), sulfate (SO_4^{2-}) was measured by the turbidimetric method (Digital Nephlo-turbidity meter, Systronics-132); UV-Vis spectrophotometer (Systronics-117) was used to determine nitrate (NO_3^-) (Bruccine method) & iron (Fe^{2+}) by 1-10 phenanthroline method. Microprocessor-based flame photometer (EI-1381) was used to analyze sodium (Na^+), potassium (K^+), calcium (Ca^{2+}), magnesium (Mg^{2+}) and lithium (Li^+). Demineralized water was used to prepare the standard and working solutions.

The USGS modular hydrologic model MODFLOW, version 4, was used to simulate the groundwater flow and classify water types by creating a Piper diagram. A Gibbs diagram was generated to analyze the water quality and understand geochemical processes using a geochemical modeling program, PHREEQC, developed by the USGS and provided by the Aqua-Chem trial version of Waterloo Hydrogeologic.

2.4.2 Rock samples

Rock samples from both blocks of the district were collected by the grab sampling method. The elemental compositions of the rock samples were analyzed via SEM via Oxford energy dispersive X-ray spectroscopy (EDXS, INCA 250 EDS with an X-MAX 20 mm Detector).

3. RESULTS AND DISCUSSION

3.1 Major ion chemistry

Analyzing the major ions (Na^+, K^+, Ca^{2+}, Mg^{2+}, Cl^-, CO_3^{2-}, HCO_3^-, SO_4^{2-} and NO_3^-) is essential for understanding the hydrochemical characteristics of groundwater (Gao et al., 2019). A statistical analysis of 32 groundwater samples collected during both seasons revealed fluoride concentrations varying between 0.28 and 4.0 mg/L during the PRMS, with a mean value of 0.95 mg/L (+0.71 SD). The fluoride concentrations in the POMS varied between 0.34 and 6.2 mg/L, with a mean of 1.37 (+1.26 SD) (Table 1). The concentration of fluoride in drinking water in some places exceeded the WHO permissible limit of 1.5 mg/L (WHO 2011). In both seasons, in the Mainpur block, 11% of the water samples had fluoride levels exceeding the permissible level, while, in the Devbhog block 5% of the water samples had fluoride levels above the permissible level during the PRMS, and 22% of the samples had fluoride levels above the permissible level in the POMS.

Table 1. Statistical analysis of water samples collected during the PRMS and POMS

	pH	EC (mS)	F^-	Cl^-	SO_4^{2-}	TH	Ca	Mg	Fe^{2+}	HCO_3	ORP (mV)	DO (mV)	TDS	Na^+	K^+	Li^+	Sal (ppt)
Max	7.4[a] 7.2[b]	0.71 0.64	4.0 6.2	106 213	15.1 15.2	244 270	83.2 70.4	59.5 65.9	0.19 0.17	95 75	98 596	5.6 7.3	317 501	98.7 100	2.1 3.2	0.2 0.2	400 500
Min	6.1[a] 5.9[b]	0.26 0.33	0.28 0.34	38 67.2	3.5 3.5	108 101	37.6 33.2	26.3 22.4	0.05 0.01	15 25	109 13	1.1 1.4	105 160	16.7 10.6	0.1 0.1	0 0	100 100
Mean	6.6[a] 6.1[b]	0.48 0.45	0.95 1.37	72.4 131	6.6 6.1	144 134	50.9 46.3	35.5 32.4	0.09 0.07	50 48	46 296	2.0 4.2	246 294	74.5 48.5	0.83 1.5	0.07 0.05	200 300
SD	0.35[a] 0.63[b]	0.13 0.08	0.71 1.26	15.7 41.7	2.20 2.16	27 31	9.15 9.0	6.9 7.7	0.04 0.04	16.9 13.4	19.9 0.06	0.96 1.4	66.6 1.46	17.5 0.01	0.55 0.85	0.06 0.07	90 90
CV	5.3 10.3	27 17.7	74.7 91.9	21.6 31.8	33.3 35.4	18.7 23.1	17.9 19.4	19.4 23.7	44.4 57.1	33.8 27.9	43.2 0.02	48 33.3	27 0.49	23.4 0.02	66.2 56.6	85.7 140	45 30
MDL	6.5	-	1.0	200	200	200	75	50	0.3	-	200-600	-	500	-	-	0.70	500-2000
MPL	8.5	-	1.5	600	400	600	200	150		-	800	5	1500	200	12	0.70	-

% SMPL	-	-	12.5[a] 9.4[b]	-	-	-	84.3 100	9.37 -	-	-	-	31.2 40.6	-	-	-	-	-

SD- Standard deviation; CV- Coefficient of variation; MDL- maximum desirable limit; MPL- maximum permissible limit; %SMPL- percentage of samples exceeding maximum permissible limit; a-pre-monsoon season; b- post-monsoon season. (Ca and Mg are reported as $CaCO_3$) All the units are in mg/L or otherwise mentioned.

Na^+ is the dominant cation in the study region, with a mean of 74.5 mg/L in PRMS and 48.5 mg/L in POMS. The dissolution of halite and silicate may increase the concentration of Na^+ in aqueous solution (Li et al., 2016). The concentration of Ca^{2+} initially decreased from the Devbhog block toward the midstream region, the Telnadi River, with an increasing value toward the slope, i.e., Mainpur block (Beg, et al., 2023) with a mean value of 50.9 mg/L during PRMS and 46.3 mg/L in POMS. Exceedingly high concentrations of fluoride in the underground waters of the Devbhog block in both the seasons i.e. pre-monsoon (4.0 mg/L) and post-monsoon (6.2 mg/L) might be due to the cation exchange mechanism between Na^+ in aqueous solution with fluorite (CaF_2) in sediments (Zaidi et al., 2015). During the PRMS dissolved oxygen (D.O.) concentration was less (1.1-5.6 mg/L) which induced the formation of bicarbonate ions in the deep aquifer through the condensation of geothermal steam (Hanor & Wendeborn, 2023). High concentrations of HCO_3^- ions in the PRMS (15-95 mg/L) caused precipitation of Ca^{2+} in the form of calcium carbonate (Juarez et al., 2023), which led to the dissolution of fluoride from fluorite minerals in the groundwater (Hu et al., 2021). The reaction of sodium bicarbonate with fluorite mineral promotes increased F^- levels in groundwater (eq.1) (Capuano & Jones, 2020).

$$\boldsymbol{CaF_2 + 2NaHCO_3 = CaCO_3 \downarrow + 2NaF + 2H^+ + CO_3^{2-}} \qquad \textbf{(1)}$$

A high fluoride concentration in the Devbhog block during the pre-monsoon season can be justified by understanding the equilibrium reaction (eq. 2) of F^- under neutral pH conditions.

$$\boldsymbol{Ca^{2+} + 2HCO_3^- = CaCO_3 \downarrow + H_2CO_3} \qquad \textbf{(2)}$$

The weathering of calcite and dolomite in the metamorphic rocks of the region under high tropical climatic conditions also contributed to increased levels of bicarbonate ions in the groundwater (Sharma & Sharma, 2021). When calcite and fluorite reach their equilibrium solubility, they create a stable interaction that highlights the importance of understanding mineral solubility in our environment (Nordstrom, 2022), as shown in equation 3.

$$\boldsymbol{CaF_2 + HCO_3^- = CaCO_3 + 2F^- + H^+} \qquad \textbf{(3)}$$

The saturation of calcite and its precipitation are imperative for an increased fluoride concentration. Additional sources of bicarbonate alkalinity actively promote calcite precipitation at a specific pH. Statistical analysis of the water samples revealed the general dominance of cations $Na^+ > Ca^{2+} > Mg^{2+} > K^+$ in groundwater during the pre- and post-monsoon periods. Among anions, the concentration of chloride

(Cl^-) was the most uneven among all anions, ranging between 38 and 107 mg/L in the PRMS and 67.1 and 213 mg/L in the POMS, followed by HCO_3^->SO_4^{2-}>F^- (Table 1). The concentrations of NO_3^- and PO_4^{3-} did not exceed 0.02 mg/L and 0.035 mg/L, respectively. This indicated the ions were not generated by agricultural activities predominating in the area.

Box and Whisker plot

A Box and Whisker plot of ions are illustration used to display multiple comparisons in a graph. In Devbhog, the Q1 value (25% of samples below this point) for Cl^- ion is 80 mg/L, which is higher than in Mainpur (70 mg/L). Likewise, Q3 value (75% of samples below this point) is also higher 158.5 mg/L, than in the Mainpur block (106.5 mg/L) as shown in Figure 2. The higher Inter Quartile Range (IQR) of Cl^- ion (78.8 mg/L) in Devbhog indicates its major distribution in the groundwater compared to Mainpur (35 mg/L). The concentration of HCO_3^- is higher (95 mg/L) in Mainpur, indicated by the length of the whisker extending farther away from the median. The maximum value of Ca^{2+} ions (105 mg/L) in Devbhog block is again higher than in Mainpur (67.2 mg/L) as evidenced by the whisker's length. The Q1 value for Na^+ ion in Mainpur block is 58.7 mg/L and a median of 76 mg/l, which is higher compared to Q1 (16 mg/L) and median values (56 mg/L) in Devbhog. This indicates that more than 25% of the samples in Mainpur have a greater concentration of Na^+ ions dissolved in the groundwater.

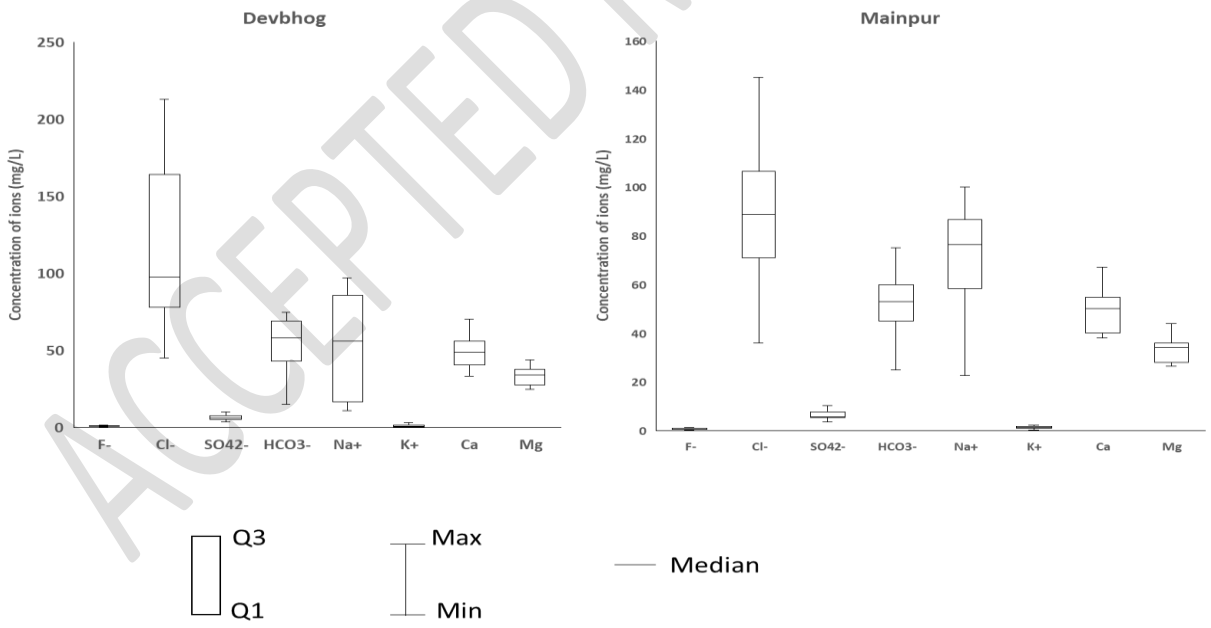

Fig. 2 Box and Whisker plots of major ionic concentrations

Pearson Correlation

To estimate the linear relationship between the bivariate parameters (F^- and other ions), Pearson correlation analysis was performed, and Table 2 shows that during the PRMS, fluoride ion showed significantly low positive correlation with (HCO_3^- & Na^+) showed by strength of bivariate relationship, the correlation coefficient (r<0.1); *p*<0.001. It showed weakly negative correlation with (Fe^{2+}&TDS) (r<-0.2) and poorly negative correlated with (Cl^-, SO_4^{2-}, Ca^{2+}, Mg^{2+}, CO_3^{2-} & ORP) (r<-0.1). In the dry season, the evaporative concentration of salts increases, as supported by a low but significant positive correlation between F^- and EC (r=0.05). Higher concentrations of Na^+ in PRMS tend to have greater concentrations of soluble fluoride (NaF) in groundwater but under neutral pH conditions F^- is exchanged with Ca^{2+} ions of fluorapatite minerals in rocks (Egor & Birungi 2020) thus a reducing level of fluoride in the water sample was observed.

During the POMS, fluoride concentrations showed significantly strong correlation with Ca^{2+}, OH^-, and Li^+ (r>0.6); *p*< 0.001, was weakly correlated with Mg^{2+}, Cl^- and Fe^{2+}(r= 0.3-0.4); poorly correlated with Na^+ and HCO_3^- (r< 0.3); and negatively correlated with only K^+ (r= -0.25) (Table 3). This result is also supported by high fluoride levels in the Devbhog district, which has low concentrations of sodium in groundwater (Bhattacharyya et al., 2022). A significant positive correlation of fluoride with Ca^{2+} and CO_3^{2-} was observed. This indicates rainwater carrying dissolved CO_2 percolates inside the earth's surface during POMS. This water reacts with calcite to form bicarbonate and calcium ions (eq. 4).

$$\boldsymbol{CaCO_3 + H_2O + CO_2 = Ca^{2+} + HCO_3^-} \qquad \textbf{(4)}$$

The increased alkalinity (OH^-, CO_3^{2-}, HCO_3^-) of the groundwater during POMS is also responsible for the decreased sodium concentration in the aqueous solution, as shown in equation 5 (Sar et al., 2020). Sodium is present in aqueous solution as partially soluble sodium bicarbonate.

$$\boldsymbol{NaOH + H_2O + H_2CO_3 = NaHCO_3} \qquad \textbf{(5)}$$

Under alkaline conditions the primary mineral sources like fluorite, biotite and amphibolite releases fluoride in water (Jia et al., 2019).

Table 2. Pearson Correlation matrix of fluoride with various ions in PRMS

	pH	EC	F-	Cl-	SO4	Ca2+	Mg2+	TH	Fe2+	HCO3-	NO3-	PO4	Na+	K+	Li+	ORP	DO	TDS	Sal
pH	1.00																		
EC	-0.21	1.00																	
F-	0.32	0.05	1.00																
Cl-	0.19	-0.26	-0.12	1.00															
SO4	-0.12	0.40	-0.07	-0.14	1.00														
Ca2+	0.12	0.15	0.01	0.24	0.27	1.00													
Mg2+	0.08	0.24	-0.03	0.18	0.37	0.95	1.00												
TH	0.04	0.17	-0.02	0.25	0.32	0.95	0.97	1.00											
Fe2+	0.04	0.18	-0.11	0.22	0.50	0.21	0.24	0.21	1.00										
HCO3-	0.25	-0.18	-0.05	0.52	-0.16	-0.15	-0.14	-0.08	0.16	1.00									
NO3-	0.12	0.23	0.06	0.24	0.04	0.48	0.49	0.50	-0.12	-0.03	1.00								
PO4	0.07	0.28	0.03	0.13	0.11	0.30	0.35	0.33	-0.02	0.12	0.73	1.00							
Na+	0.02	-0.07	0.01	0.05	0.27	-0.27	-0.23	-0.22	0.40	0.28	-0.43	-0.41	1.00						
K+	-0.09	0.35	0.11	-0.08	0.17	-0.30	-0.14	-0.17	0.12	0.21	0.14	0.24	0.30	1.00					
Li+	-0.02	0.46	0.07	-0.41	0.35	0.07	0.20	0.09	0.04	-0.34	0.17	0.47	-0.05	0.27	1.00				
ORP	-0.09	0.30	-0.21	-0.09	0.40	0.58	0.60	0.61	0.10	-0.20	0.34	0.36	-0.28	-0.26	0.31	1.00			
DO	0.01	-0.23	-0.10	0.54	-0.26	-0.21	-0.20	-0.16	0.07	0.72	-0.10	0.15	0.13	0.25	-0.35	-0.41	1.00		
TDS	-0.17	0.30	-0.05	-0.25	0.10	0.20	0.16	0.15	0.11	-0.46	0.10	0.03	-0.29	-0.30	0.07	0.55	-0.56	1.00	
Sal	-0.07	-0.02	-0.22	-0.03	0.19	0.42	0.42	0.46	0.08	-0.06	0.38	0.30	-0.28	0.06	-0.01	0.53	0.01	0.13	1.00

Table 3 Pearson Correlation matrix of fluoride with various ions in POMS

	pH	EC	F-	Cl-	SO4	Ca2+	Mg2+	TH	Fe2+	OH-	CO3	HCO3-	NO3-	PO4	Na+	K+	Li+	ORP	DO	TDS	Salinity
pH	1.00																				
EC	-0.16	1.00																			
F-	0.39	0.24	1.00																		
Cl-	0.30	0.36	0.32	1.00																	
SO4	-0.12	0.42	0.32	0.53	1.00																
Ca2+	0.15	0.38	0.54	0.07	0.22	1.00															
Mg2+	0.15	0.29	0.43	0.05	0.16	0.87	1.00														
TH	0.18	0.22	0.42	0.03	0.14	0.87	0.97	1.00													
Fe2+	0.46	0.11	0.30	0.32	0.08	0.08	0.01	-0.03	1.00												
OH-	0.33	0.25	0.70	0.20	0.13	0.49	0.27	0.27	0.45	1.00											
CO3	0.33	0.12	0.63	0.07	0.04	0.68	0.76	0.77	0.25	0.70	1.00										
HCO3-	0.43	0.19	0.26	0.10	-0.19	0.11	0.01	0.04	0.06	0.02	-0.02	1.00									
NO3-	0.07	0.02	0.21	-0.03	0.15	0.00	-0.04	0.03	-0.14	-0.01	-0.01	-0.01	1.00								
PO4	-0.18	0.59	0.17	0.29	0.01	0.24	0.16	0.11	0.24	0.22	0.15	0.11	0.04	1.00							
Na+	-0.40	0.20	0.14	-0.28	0.16	-0.06	-0.10	-0.13	-0.47	-0.18	-0.26	0.02	0.43	-0.02	1.00						
K+	0.07	0.09	-0.25	0.21	0.08	-0.50	-0.39	-0.43	0.09	-0.30	-0.43	-0.15	0.21	0.01	0.14	1.00					
Li+	0.46	0.09	0.67	0.16	0.01	0.51	0.56	0.54	0.24	0.43	0.62	0.44	0.00	0.24	-0.10	-0.47	1.00				
ORP	0.48	0.01	0.11	0.26	-0.20	-0.15	-0.05	-0.04	0.25	0.06	0.11	0.38	-0.27	-0.08	-0.27	0.37	0.04	1.00			
DO	0.65	-0.18	0.28	0.18	-0.19	-0.19	-0.16	-0.17	0.23	0.00	-0.06	0.39	0.14	-0.15	0.04	0.43	0.18	0.68	1.00		
TDS	0.42	0.03	0.10	0.38	0.08	-0.22	-0.19	-0.19	0.03	-0.02	-0.17	0.14	0.17	-0.29	0.09	0.48	-0.06	0.49	0.60	1.00	
Salinity	0.36	-0.01	0.22	0.35	0.08	0.04	0.12	0.15	0.12	0.11	0.16	-0.01	0.24	-0.16	-0.04	0.29	0.18	0.35	0.46	0.48	1.00

3.2 Depth of handpumps and Ionic concentrations

The direction of groundwater flow in the Gariyaband district is toward the slope of the district, i.e., from the Devbhog block (south) toward the Mainpur block (north), which is indicated by the physiography of the district (Manjhi, 2019). Table 4 indicates the depth of hand pumps in the sampling area. All the hand pumps in the Devbhog block were much deeper (93.6–127.2 m) then the Mainpur block (72.9-96.3 m). The concentrations of all the cations and anions including F^- ion in the groundwater were reportedly high in the Devbhog block as evidenced from the box-plot study. This is because underground water at greater depths has a longer contact time with subsurface rocks. This causes a greater chance of the dissolution of minerals from the parent rock into the aqueous solution (Winter et al., 1998).

Table 4. Depth of hand pumps at sampling locations in two blocks

S. No.	Block	Sampling Site	latitude	Longitude	Depth of hand pump (meters)	Avg. F^- conc. (mg/L)
1	Mainpur	Tawrenga	20.16379	82.25208	77.4	0.85
2		Taurenga	20.1451	82.27408	72.9	0.62
3		Jugad	20.1368	82.27061	78.3	0.43
4		Mainpur	20.1332	82.28413	81.9	0.34
5		Jangada	20.11988	82.29307	76.8	0.95
6		Udanti	20.10122	82.29593	84.9	1.1
7		Indagaon	20.08777	82.33302	78.6	0.98
8		Kandsar	20.01422	82.37677	94.5	1.2
9		Khokhma	19.99956	82.37381	96.3	0.95
10		Ladhwapara	20.00248	82.41994	91.5	0.86
11		Dhurwagudi	19.98235	82.4455	96.6	0.59
12		Dharnidho	19.9966	82.45922	92.4	1.1
13		Nawagaon	19.96866	82.46778	89.1	0.28
14		Madangmuda	19.99537	82.29575	94.2	3.3
15		Gohrapadar	19.98335	82.48444	86.4	3.2
16		Mahulkot	19.94476	82.57483	94.8	0.82
17		Mudagaon	19.8775	82.65121		1.3
18	Devbhog	Tel River	19.90351	82.62686	98.4	1.7
19		Dohel	19.9137	82.60941	106.2	0.83
20		Deobhog	19.91555	82.55121	102.3	0.67
21		Jharaban	19.90877	82.6142	110.7	0.55
22		Kurmibasa	19.90703	82.63015	93.6	0.35
23		Dabnai	19.90522	83.64815	98.4	0.94
24		Dahigaon	19.89116	82.62838	93.3	0.68
25		Kumhdaikhurd	19.89443	82.62725	101.7	0.34
26		Kosamkani	19.8878	82.61494	110.1	0.94
27		Kodobeda	19.89205	82.6643	112.2	0.95
28		Madagaon	19.8852	82.65313	115.2	1.03
29		Navaguda	19.88748	82.62529	109.2	1.16
30		Fulimuda	19.87812	82.61237	116.1	1.2
31		Nisthiguda	19.88507	82.6607	120.6	4.85
32		Supebeda	19.87921	82.67608	127.2	1.5

3.3 Water types (Piper plot)

To determine the water quality of the area by analyzing dissolved constituents and thereby classifying

them into various facies based on relative abundance, a Piper diagram was generated from the experimental data (Fig. 3). The cations (Na^+, K^+, Ca^{2+}, and Mg^{2+}) and anions (Cl^-, HCO_3^-, and SO_4^{2-}) in the milliequivalent concentration were plotted in a ternary diagram to determine the relationships between ions in the water samples. During the PRMS, 80% of the groundwater samples contained alkaline earth metals (Ca^{2+}+Mg^{2+}), while only 20% of water samples had alkali (Na^++K^+) concentrations greater than alkaline earth metals. A similar trend was also observed during POMS, where 68% of the samples had greater alkaline composition, while 32% of the samples had higher concentrations of alkali metals (Table 5). Only 3% of the samples indicated the dominance of strong acid (SO_4^{2-}+Cl^-) over weak acid (HCO_3^-) in the PRMS, while during the POMS, the concentration of strong acid exceeded that of weak acid in all the samples. Overall, during PRMS, a smaller percentage of the water samples revealed noncarbonated hardness/alkali facies, while in all the samples, noncarbonated hardness/alkali facies dominated during the POMS. Based on these findings, the groundwater from these two districts was classified as Ca-Mg- HCO_3^- type water in PRMS, while Ca-Mg-Cl-type water in POMS. A similar hydrogeochemical study from East Jinan City of China reported weathering and simultaneous dissolution of rock as the major hydrochemical processes operating in the region (Zhang et al., 2018).

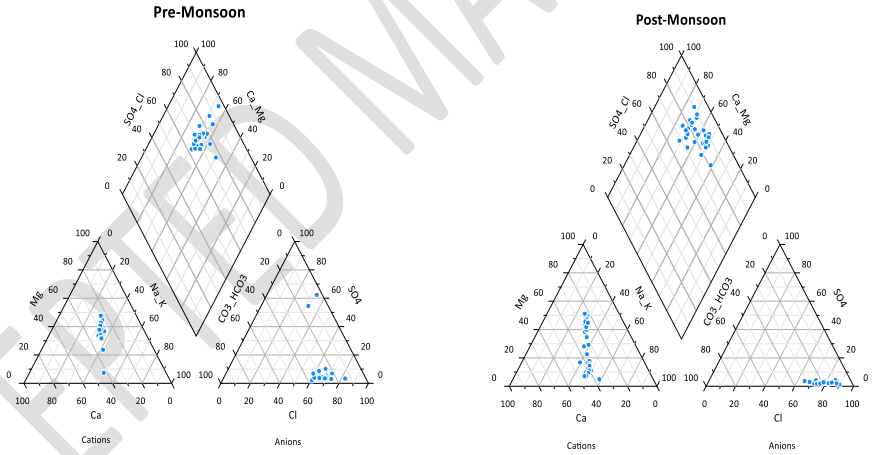

Fig 3. Piper diagram of groundwater samples

Table 5. Groundwater samples showing the type of water according to the Piper plot

S.No.	Characteristic of water samples according to Piper plot	% of groundwater samples showing characteristics during	
		PRMS	POMS
1.	Alkaline earth (Ca+Mg) exceeding Alkali (Na+K)	80	68
2.	Alkali (Na+K) exceeding Alkaline earth (Ca+Mg)	20	32

3.	Strong acid (SO_4+Cl) exceeding Weak acid(HCO_3)	3	100
4.	Non-carbonate hardness exceeding Carbonate hardness	3	100
5.	Non-carbonate alkali exceeding Carbonate Alkali	3	100

3.4 Hydrochemical Processes

The Gibbs diagram is widely used to establish the relation between aquifer chemical composition and lithological characteristics of an area and to understand the natural mechanism (Gibbs, 1970). In this method, the TDS concentration is plotted against the ratio of $(Na^+)/(Na^+ + Ca^{2+})$ for positively charged ions and $(Cl^-)/(Cl^- + HCO_3^-)$ for negatively charged ions. The Gibbs diagram illustrates the mechanisms functioning in nature, such as rock weathering and evaporation/precipitation processes, which regulate the groundwater chemistry of an area (Khan & Jhariya, 2018). The value of $(Na^+)/(Na^+ + Ca^{2+})$ between 0.4 and 0.9, and for $(Cl^-)/(Cl^- + HCO_3^-)$ between 0.6 and 0.9 in Figure 4a with TDS varying between105-317 mg/L indicates that Mainpur block is dominated by silicate minerals in the rock and Na-Cl type facies in the groundwater (Marandi & Shand, 2018; Rugner et al., 2013). Since most of the samples fall on the right side of the graph, it indicates that evaporation and sedimentation factors are responsible for the governing chemical composition of water. In Devbhog, the lower value of $(Na^+)/(Na^+ + Ca^{2+})$ between 0.1 to 0.2 and a higher value of $(Cl^-)/(Cl^- + HCO_3^-)$ between 0.6 to 0.9 as shown in Figure 4b with TDS varying between 160-501mg/L indicates Ca-Cl type water with increased salinity in Devbhog. The Gibbs diagram for the water samples from Devbhog indicated a predominance of rock, showing rock-water interaction and mineral dissolution process controlling the hydrochemistry of the region (Nazzal et al., 2014). In Mainpur block, the chemical characteristics of groundwater is due to evaporation-condensation processes dominating the region. A similar result is reported by Gaikwad et al (2018) in a hydrogeochemical study on the upper Bhima Basin of Western India, having semi-arid climatic conditions.

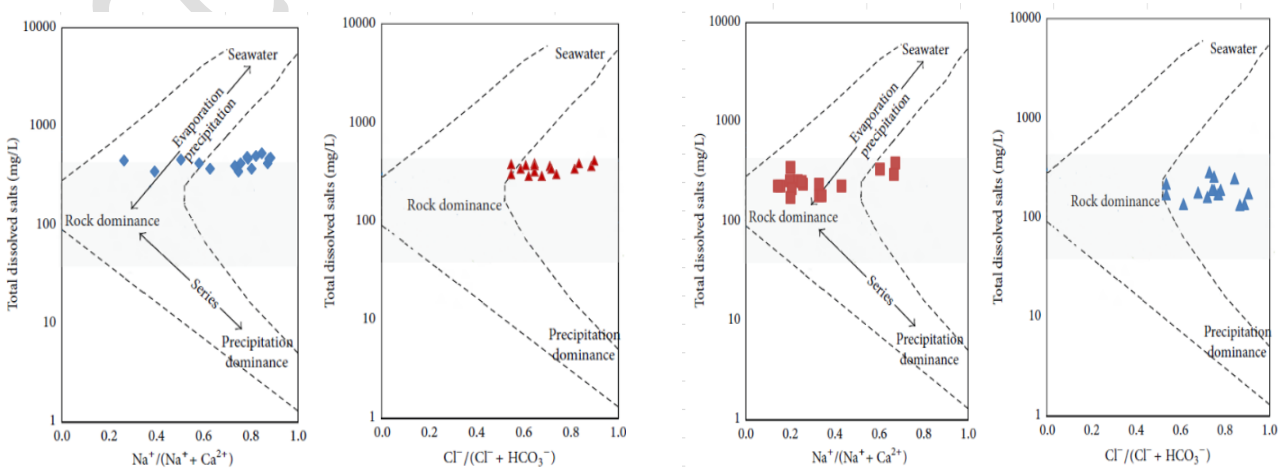

Fig. 4a. Gibbs diagram showing a plot of TDS versus (Na/Na+Ca) and TDS versus (Cl/Cl+HCO_3) to study the dominant process controlling groundwater chemistry in the Mainpur block

Fig. 4b. Gibbs diagram showing a plot of TDS verses (Na/Na+Ca) and TDS verses Cl/Cl+HCO_3) to study the dominant process controlling groundwater chemistry in the Devbhog block

Chloro-alkali indices

To understand the ion exchange reactions between groundwater and clay minerals in aquifers/parent rocks, hydrochemical data are plotted in equations 6 and 7, representing groundwater's chloro-alkali indices (CAIs) (H. Schoeller, 1967). The two chloro-alkali indices are expressed as follows:

$$\textbf{CAI-I} = [Cl^- - (Na^+ + K^+)]/Cl^- \textbf{ (meq/L)} \quad (6)$$

$$\textbf{CA-II} = [Cl^- - (Na^+ + K^+)]/(SO_4^{2-} + HCO_3^- + NO_3^-) \textbf{ (meq/L)} \quad (7)$$

A positive value for both indices (Table 6) indicates chloro-alkaline disequilibrium or a reverse cation-anion exchange process (eq. 9). In contrast, a negative value suggests base exchange reactions (eq. 8) regulating the aqueous matrix (Tarawneh et al., 2019).

1. Base exchange reaction

$$Na^+ + HCO_3^- + [(Ca^{2+} - Mg^{2+}) - sediment] = (Ca^{2+} - Mg^{2+})CO_3^- + H_2O + (Na^+ - sediment) \quad (8)$$

2. Chloro-alkaline disequilibrium (reverse base exchange)

$$(Ca^{2+} - Mg^{2+})CO_3^- + H_2O + (Na^+ - sediment) = Na^+ + HCO_3^- + [(Ca^{2+} - Mg^{2+}) - sediment] \quad (9)$$

During the PRMS, the CAI-I values ranged from -0.04 to 2.25, with a mean value of 0.41 in the groundwater samples from both blocks (Table 6); comparatively, the CAI-II values ranged between -0.21 and 1.75, with a mean value of -1.2. Collectively, 69% of the water samples had positive CAI-I values, while 81.2% had negative CAI-II values. This indicates that during PRMS, base exchange reactions are dominant increasing the concentration of Ca^{2+} and Mg^{2+} in water and sodium ions deposited in sediments. This decreased the fluoride concentration, as it formed the insoluble ionic compound CaF_2 in groundwater (Ropp, 2012).

In POMS the CAI-I values ranged from -0.07 to 5.41, with a mean value of 3.04 in all the groundwater samples from both blocks, and CAI-II values ranged from -0.01 to 4.49, with a mean of 1.31. Notably, 99% of the water samples had positive CAI-I indices, while 62.5% had positive CAI-II values. This elucidated reverse base exchange reactions predominate in the region; i.e., Ca^{2+} and Mg^{2+} in water samples were exchanged with the Na^+/K^+ ions in sediment/rock (Gantait et al., 2022). This increased the fluoride concentrations (NaF) in water (Krishna Kumar et al., 2014).

Table 6. Gibbs ratio, CAI-I and CAI-II for assessing groundwater quality

S. No.	Sampling Locations	$(Na^+)/(Na^+ + Ca^{2+})$	$Cl^-/(Cl^- + HCO_3^-)$	CAI-I (PRMS)	CAI-II (PRMS)	CAI-I (POMS)	CAI-II (POMS)
1	Tawrenga	0.17	0.61	-0.08	-2.07	1.68	0.02
2	Taurenga	0.14	0.58	0.79	-0.81	1.30	0.27
3	Jugad	0.15	0.73	0.72	-1.19	0.84	-2.06
4	Mainpur	0.17	0.64	0.61	-1.48	1.11	-1.34
5	Jangada	0.24	0.54	0.49	-1.52	-0.07	-1.84
6	Udanti	0.19	0.60	0.69	-1.49	2.01	-0.84
7	Indagaon	0.05	0.70	0.43	-1.23	2.32	0.27
8	Kandsar	0.23	0.64	0.13	-2.68	1.11	-2.71
9	Khokhma	0.22	0.54	-0.12	-2.13	-0.07	-3.48
10	Ladhwapara	0.20	0.71	-2.38	-4.12	4.45	-0.01
11	Dhurwagudi	0.07	0.67	-1.38	-3.08	4.85	3.86
12	Dharnidho	0.12	0.88	-0.70	-2.16	2.49	-0.18
13	Nawagaon	0.21	0.81	0.04	-2.92	3.29	-0.70
14	Madangmuda	0.22	0.83	-0.11	-2.08	5.37	1.96
15	Gohrapadar	0.26	0.64	1.26	0.57	1.60	-1.12
16	Mahulkot	0.25	0.89	1.18	0.14	2.35	-1.05
17	Mudagaon	0.29	0.54	-0.08	-1.86	-0.08	-1.86
18	Tel River	0.25	0.74	0.94	-0.52	5.41	3.04
19	Dohel	0.05	0.76	-0.83	-2.93	3.92	3.45
20	Deobhog	0.05	0.78	0.82	-0.75	4.73	4.21
21	Jharaban	0.07	0.90	0.71	1.42	3.56	2.86
22	Kurmibasa	0.21	0.85	0.78	1.61	4.94	3.83
23	Dabnai	0.05	0.79	0.94	-0.58	3.90	3.24
24	Dahigaon	0.06	0.92	1.64	-2.25	4.57	3.58
25	Kumhdaikhurd	0.15	0.54	0.82	-0.21	3.23	2.73
26	Kosamkani	0.04	0.76	0.67	-0.21	3.94	3.51
27	Kodobeda	0.09	0.69	-1.14	-2.22	4.57	4.27
28	Madagaon	0.07	0.62	1.04	-1.41	3.52	3.19
29	Navaguda	0.07	0.75	-0.04	-1.78	4.48	4.07
30	Fulimuda	0.04	0.73	1.31	-0.59	4.20	3.94
31	Nisthiguda	0.03	0.78	1.72	0.14	4.95	4.49
32	Supebeda	0.09	0.88	2.25	1.75	2.89	2.50

3.5 Mineralogical study of the region

The northern part of the study area covering Mainpur is underlain by rocks of the Bengpal Group (metasedimentary rocks) mainly consisting of sandstone, schist and shale (CGWB, 2022; Dora et al., 2021). In contrast, Devbhog in the southeastern part of the district consists of rocks from the Chandrapur Group, such as gneiss, charnokite-khondalite, migmatite, and schist rocks (Sahoo, 2013). The region's hydrology reveals that major aquifer systems in the two blocks are beneath deep fractured hard crystalline rocks with gneissic forms (Kaur, 2023). The groundwater quality of an area is an amalgamation of geomorphological and climatic conditions in addition to saturated infiltration from the soil to the bedrock (Katsura et al., 2008).

The morphological characterization of the igneous rocks from the Mainpur block was carried out via SEM (Fig. 5a). The EDX scan of the rock (Fig. 5b) revealed that the major elements were Si (24.69%) and O (52.69%), others were Ca (7.7 wt%), K (4%), Cl (3%), P (2.3%), Na (2.19%), Mg (1.53%), and Al (1.79%). This confirms the presence of halite (NaCl), alkali feldspar $(SiAl)O_4$, apatite $(Ca_{10}(PO_4)_6X_2)$, Al, Ca-rich plagioclase and felsic minerals (Na-rich feldspar) in the siliclastic rocks of the region

(Graham, 2018). SEM images of the metamorphic rocks from the Devbhog block are shown in (Fig. 5c). The EDX scan of the rock (Fig. 5d) revealed that the major elements were Si (19.65%), O (56.35 wt%), Ca (7.5 wt.%), K (2.43 wt%), C (4.82 wt%), Al (3.08%), Fe (2.41%), and Mg (1.76%). The metamorphic rocks with low silica contents enriched in iron and magnesium indicate the presence of gneissic minerals, fluorite (CaF_2), cryolite (Na_3AlF_6), calcite ($CaCO_3$), dolomite $CaMg(CO_3)_2$, fluorapatite ($Ca_5(PO_4)_3$ and muscovite ($KAl_2(AlSi_3O_{10})(OH)_2$ in the block (Le Bas & Streckeisen, 1991). These minerals contribute to dissolution, precipitation and ion-exchange processes, resulting in elevated fluoride concentrations in the study area (Kumar, P. et al 2019).

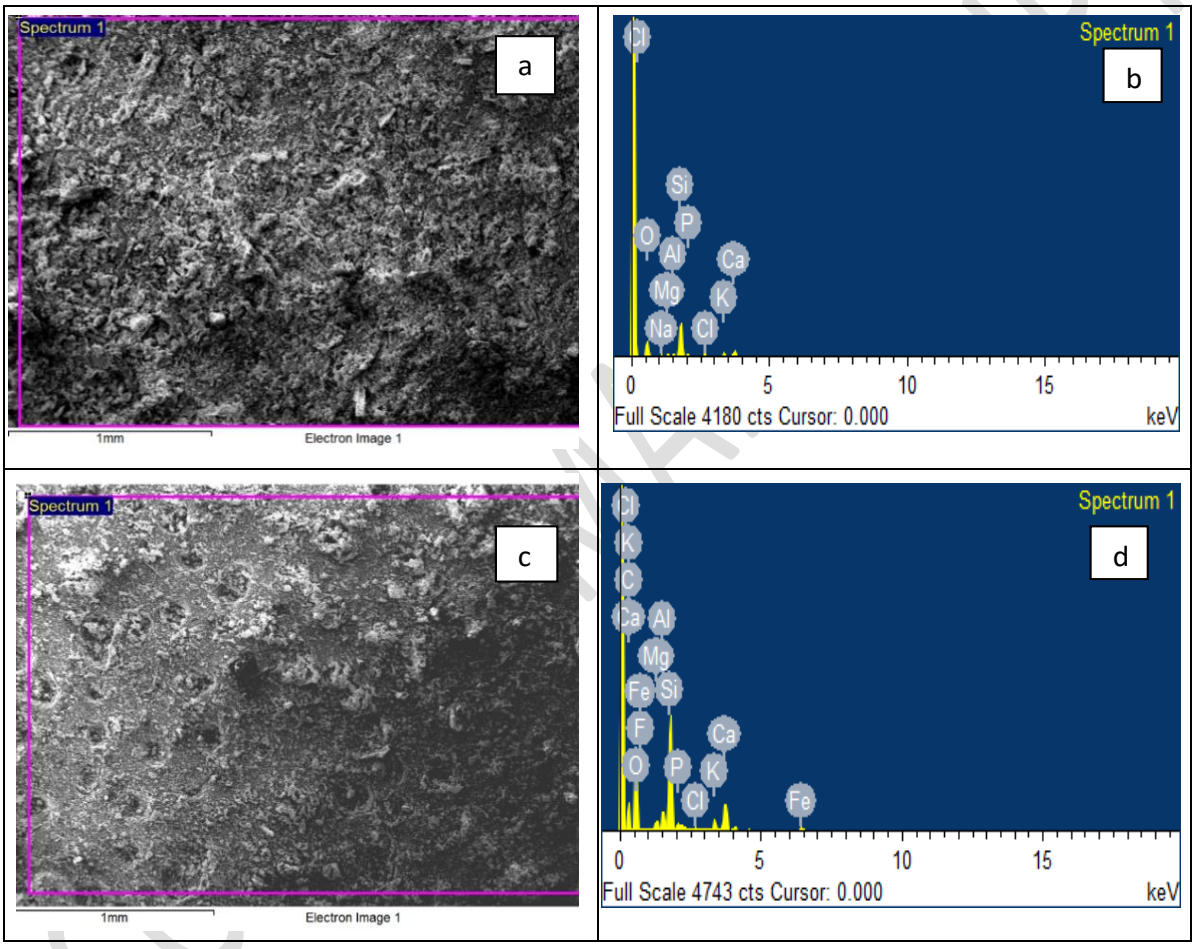

Fig. 5. a) and b) SEM and EDX characterization of rocks from Mainpur block
c) and d) SEM and EDX characterization of rocks from Devbhog block

4. CONCLUSION

In the tropical climate of the Gariyaband district, groundwater samples were analysed during pre- and post-monsoon seasons from the Mainpur and Devbhog blocks to assess fluoride contamination in drinking water tapped from handpumps. Box-Whisker plot revealed that Devbhog block is dominated by Ca^{2+} and Cl^- ions while in Mainpur Na^+ and Cl^- ions predominate, highlighting the unique

characteristics of this region's groundwater. Notably, a significant fluoride concentration of 6.2 mg/L was observed in the groundwater samples collected during the post-monsoon season from Devbhog. This elevated level of fluoride may likely be due to the precipitation of calcium as carbonate ($CaCO_3$), as explained by chloro-alkaline disequilibrium reactions dominant during POMS, which facilitates the release of soluble fluoride into the groundwater. This presents a complex picture of the hydrological dynamics in the area. During PRMS, under slightly alkaline groundwater conditions, calcium precipitated in sediments, releasing fluoride ions from fluorite minerals to a lesser extent (4.0 mg/L) than POMS. Rock weathering and mineral dissolution processes are the primary geochemical processes that control groundwater chemistry and fluoride enrichment in Devbhog, while evaporation and sedimentation govern the hydrochemistry of Mainpur block.

ACKNOWLEDGMENTS

I acknowledge Thakur Vikram Singh from the School of Studies in Environmental Science, Pt. Ravishanker Shukla University, Raipur, C.G., India, for projecting the map of sampling locations through ArcGIS software.

FUNDING DECLARATION

We are thankful to the Chhattisgarh Council of Science and Technology for granting and funding this mini-research project (2543/CCOST/MRP/2017)

CONFLICT OF INTEREST

The authors declare that there is no conflict of interest regarding the publication of this manuscript.

REFERENCES

APHA (2017). Standard Methods for the Examination of Water and Wastewater (23rd ed.). Washington DC: American Public Health Association.

Ayotte, J. D., Szabo, Z., Focazio, M. J., & Eberts, S. M. (2011). Effects of human-induced alteration of groundwater flow on concentrations of naturally-occurring trace elements at water-supply wells. *Applied geochemistry*, *26*(5), 747-762.

Beg, M. K., Kumar, N., Srivastava, S. K., & Carranza, E. J. M. (2023). Interpretation of fluoride groundwater contamination in Tamnar area, Raigarh, Chhattisgarh, India. *Earth*, *4*(3), 626-654.

Bhattacharyya, S., Poi, R., Mandal, S., Baskey Sen, M., Hazra, D. K., Saha, S., & Karmakar, R. (2022). Method development, validation, monitoring, seasonal effect and risk assessment of

multiclass multi pesticide residues in surface and ground water of new alluvial zone in eastern India. *Environmental Science and Pollution Research*, *29*(12), 17174-17187.

Brindha, K., & Elango, L. (2011). Fluoride in groundwater: causes, implications and mitigation measures. *Fluoride properties, applications and environmental management*, *1*, 111-136.

Briscoe, J & Malik, (2005). India's Water Economy: Bracing for a Turbulent Future, The World Bank, Oxford University Press.

Capuano, R. M., & Jones, C. R. (2020). Cation exchange in groundwater-chemical evolution and prediction of paleo-groundwater flow: A natural-system study. *Water Resources Research*, 56(8), e2019WR026318.

CGWB (2022). Dynamic groundwater resources of Chhattisgarh. Groundwater survey, Water resource department, Raipur, Govt. of Chhattisgarh and CGWB, Govt. of India.

CGWB (2023). National compilation on dynamic groundwater resources of India. Dept. of water resources, Ministry of Jal Shakti, GOI, 69-70.

Chakraborty, M., Pandey, M. & Pandey, P. K. (2018). High Fluoride Concentration in Ground Water in Parts of Chhattisgarh – A Review. *International Journal of Advanced in Management, Technology and Engineering Sciences*, 8(3), 1669-1679. ISSN NO: 2249-7455.

De Giglio, O., Quaranta, A., Barbuti, G., Napoli, C., Caggiano, G., & Montagna, M. T. (2015). Factors influencing groundwater quality. towards an integrated management approach. *ANNALI DI IGIENE MEDICINA PREVENTIVA E DI COMUNITÀ*, *27*(1), 52-57.

Dhiman, S. D., & Keshari, A. K. (2006). Hydrogeochemical evaluation of high-fluoride groundwaters: a case study from Mehsana District, Gujarat, India. *Hydrological Sciences Journal*, *51*(6), 1149-1162.

Dora, M. L., Upadhyay, D., Malviya, V. P., Meshram, T., Baswani, S. R., Randive, K., Meshram, R., Suresh, G., Naik, R. & Ranjan, S. (2021). Neoarchaean and Proterozoic crustal growth and reworking in the Western Bastar Craton, Central India: constraints from zircon, monazite geochronology and whole-rock geochemistry. *Precambrian Research*, *362*, 106284.

Egor, M., & Birungi, G. (2020). Fluoride contamination and its optimum upper limit in groundwater from Sukulu Hills, Tororo District, Uganda. *Scientific African*, *7*, e00241.

Elango, L. & Kannan, R. (2007). Rock–water interaction and its control on chemical composition of groundwater. *Developments in environmental science*, *5*, 229-243.

Gaikwad, H., Shaikh, H., & Umrikar, B. (2018). Evaluation of groundwater quality for domestic and irrigation suitability from Upper Bhima Basin, Western India: a hydro-geochemical perspective. *Hydrospatial Anal*, *2*(2), 113-123.

Gantait, A., Das, S., Ghosh, S., Bohra, G., & Mukhopadhyay, S. (2022). Hydrogeochemical evolution and quality assessment of groundwater of Ajmer district, Rajasthan, India. *Journal of Earth System Science*, *131*(4), 236.

Gao, Z., Liu, J., Feng, J., Wang, M., & Wu, G. (2019). Hydrogeochemical characteristics and the suitability of groundwater in the alluvial-diluvial plain of southwest Shandong Province, China. *Water*, *11*(8), 1577.

Garcia. M. G. and Borgnino L. 2015. In Fluorine: Chemistry, Analysis, Function and Effects. ed. V. R. Preedy, The Royal Society of Chemistry. 3-21.

Gibbs, R. J. (1970). Mechanisms controlling world water chemistry. *Science*, 170(3962), 1088-1090.

Graham, I. (2018). Classification of igneous rocks.

Hanor, J. S., & Wendeborn, F. C. (2023). Origin of sodium bicarbonate groundwaters, Southern Hills Aquifer System, USA by silicate hydrolysis. *Applied Geochemistry*, *148*, 105512.

Hu, Y., You, M., Liu, G., & Dong, Z. (2021). Spatial distribution and potential health risk of fluoride in drinking groundwater sources of Huaibei, Anhui Province. *Scientific Reports*, *11*(1), 8371.

Jia, H., Qian, H., Qu, W., Zheng, L., Feng, W., & Ren, W. (2019). Fluoride occurrence and human health risk in drinking water wells from southern edge of Chinese Loess Plateau. *International Journal of Environmental Research and Public Health*, *16*(10), 1683.

Juarez, J. E. R., Alvarado, M. A. A., Zamarron, A. S., Gonzalez, O. A., Hernandez, V. H. B., Trujillo, E. O., & de Alba, Á. A. V. (2023). Chemical conditioning of drinking groundwater through $Ca^{2+/}Mg^{2+}$ ratio adjust as a treatment to reduce Ca precipitation: batch assays and test bench experiments. *Journal of Water Process Engineering*, *53*, 103844.

Kashyap, S. J., Sankannavar, R., & Madhu, G. M. (2021). Fluoride sources, toxicity and fluorosis management techniques–A brief review. *Journal of Hazardous Materials Letters*, *2*, 100033.

Katsura, S. Y., Kosugi, K. I., Mizutani, T., Okunaka, S., & Mizuyama, T. (2008). Effects of bedrock groundwater on spatial and temporal variations in soil mantle groundwater in a steep granitic headwater catchment. *Water Resources Research*, 44(9).

Kaur, G. (2023). Aquifer Mapping and Groundwater Management Plan, Gariyaband District, Chhattisgarh. Government of India, Ministry of Jal Shakti, Dept. of Water Resources, River Development and River rejuvenation, page 29-30.

Khan, R., & Jhariya, D.C. (2018). Hydrogeochemistry and Groundwater Quality Assessment for Drinking and Irrigation Purpose of Raipur City, Chhattisgarh. *Journal of the Geological Society of India,* **91**, 475–482.

Khichariya, J., & Verma, Y. (2021). Geochemistry of fluoride enrichment in groundwater: A critical review of the Indian regime. *International Journal of Chemical Engineering Research*, *8*(1), 1-4.

Krishna Kumar, S., Bharani, R., Magesh, N. S., Godson, P. S., & Chandrasekar, N. (2014). Hydrogeochemistry and groundwater quality appraisal of part of south Chennai coastal aquifers, Tamil Nadu, India using WQI and fuzzy logic method. *Applied Water Science*, 4,

Kumar, P., Meena, N.K. & Mahajan, A.K. (2019). Major ion chemistry, catchment weathering and water quality of Renuka Lake, north-west Himalaya, India. *Environmental Earth Science, 78*, 1-16.

Laxmankumar, D., Satyanarayana, E., Dhakate, R., & Saxena, P. R. (2019). Hydrogeochemical characteristics with respect to fluoride contamination in groundwater of Maheshwarm mandal, RR district, Telangana state, India. *Groundwater for Sustainable Development*, *8*, 474-483.

Le Bas, M. J. & Streckeisen, A. L. (1991) The IUGS systematics of igneous rocks, *Journal of the Geological Society,* 148(5):825-833.

Li, P., Zhang, Y., Yang, N., Jing, L., & Yu, P. (2016). Major ion chemistry and quality assessment of groundwater in and around a mountainous tourist town of China. *Exposure and Health*, *8*, 239-252.

Manjhi, P. (2019). District survey report, Gariyaband (Chhattisgarh). Directorate of geology and mining, Page 13, General profile of the district.

Marandi, A., & Shand, P. (2018). Groundwater chemistry and the Gibbs Diagram. *Applied Geochemistry*, *97*, 209-212.

Nazzal, Y., Ahmed, I., Al-Arifi, N. S., Ghrefat, H., Zaidi, F. K., El-Waheidi, M. M., Batayneh, A. & Zumlot, T. (2014). A pragmatic approach to study the groundwater quality suitability for domestic and agricultural usage, Saq aquifer, northwest of Saudi Arabia. *Environmental monitoring and assessment*, *186*, 4655-4667.

NGWA (1999). Dissolved mineral sources and significance. Chapter 23

Nordstrom, D. K. (2022). Fluoride in thermal and non-thermal groundwater: Insights from geochemical modeling. *Science of the Total Environment*, *824*, 153606.

Podgorski, J., & Berg, M. (2022). Global analysis and prediction of fluoride in groundwater. *Nature* Communications, 13(1), 4232. DOI: 10.1038/s41467-022-31940-x

Pradhanmantri Krishi Sinchayee Yojna (PMKSY) scheme, (2016). District irrigation plan Gariyaband. Page 17-18. https://pmksy.gov.in/pdflinks/SampleDIP.pdf

Reddy, A. G. S., Reddy, D. V., Kumar, M. S., & Naik, P. K. (2016). Evaluation of fluoride enrichment processes in groundwater of Chimakurthy granitic pluton complex in Prakasam District India. *African Journal of Environmental Science and Technology*, *10*(10), 350-379.

Reddy, B. M., Sunitha, V., Prasad, M., Reddy, Y. S., & Reddy, M. R. (2019). Evaluation of groundwater suitability for domestic and agricultural utility in semi-arid region of Anantapur, Andhra Pradesh State, South India. *Groundwater for sustainable development*, *9*, 100262.

Ropp, R. C. (2012). *Encyclopedia of the alkaline earth compounds*. Newnes.

Rugner, H., Schwientek, M., Beckingham, B., Kuch, B., & Grathwohl, P. (2013). Turbidity as a proxy for total suspended solids (TSS) and particle facilitated pollutant transport in catchments. *Environmental earth sciences*, *69*, 373-380.

Sahoo, M. (2013). Groundwater Brochure of Raipur district, Chhattisgarh (2012-2013). Government of India, Ministry of Water resources, Central Groundwater Board, Page-6.

Sar, S., Samuelsson, C., Engström, F., & Ökvist, L. S. (2020). Experimental study on the dissolution behavior of calcium fluoride. *Metals*, *10*(8), 988. https://doi.org/10.3390/met10080988

Schoeller, H. (1967). Geochemistry of groundwater. An International Guide for Research and Practice UNESCO, chap 15, 1–18.

Sen, I. S., & Peucker-Ehrenbrink, B. (2012). Anthropogenic disturbance of element cycles at the Earth's surface. *Environmental science & technology*, 46(16), 8601-8609.

Shankar, P. V., Kulkarni, H., & Krishnan, S. (2011). India's groundwater challenge and the way forward. *Economic and political Weekly*, 37-45.

Sharma, R. S., & Sharma, A. (2021). Metamorphism of Dolomites and Limestones. *Encyclopedia of Geology, 2nd ed.; Alderton, D., Elias, SA, Eds*, 479-491.

Sivasankar, V., Darchen, A., Omine, K., & Sakthivel, R. (2016). Fluoride: A world ubiquitous compound, its chemistry, and ways of contamination. *Surface modified carbons as scavengers for fluoride from water*, 5-32.

Suhag, R. (2016). Overview of groundwater in India. https://prsindia.org ›policy_analytical_ reports.

Tarawneh, M. S. M., Janardhana, M. R., & Ahmed, M. M. (2019). Hydrochemical processes and groundwater quality assessment in North eastern region of Jordan valley, Jordan. *HydroResearch*, *2*, 129-145.

TEL integrated multipurpose project (2008), Odisha, Government of Odisha Water Resources Department.

The Economic Times (2015). Fluoride content in water high in 17 districts of Chhattisgarh,

Tiwari, K. K., Krishan, G., Prasad, G., Mondal, N. C., & Bhardwaj, V. (2020). Evaluation of fluoride contamination in groundwater in a semi-arid region, Dausa District, Rajasthan, India. *Groundwater for Sustainable Development*, *11*, 100465.

Updated District survey Report of Gariaband (2020). Directorate of Geology and Mining Mineral Resources Department. Govt. of Chhattisgarh.

WHO (2011), Guidelines for drinking water quality. World Health Organization, Geneva.

Winter, T.C., Harvey, J.W., Franke, O.L. & Alley, W.M. (1998). Alley Ground Water And Surface Water A Single Resource, U.S. Department of the Interior, U.S. Geological Survey circular 1139.

Zaidi, F. K., Nazzal, Y., Jafri, M. K., Naeem, M., & Ahmed, I. (2015). Reverse ion exchange as a major process controlling the groundwater chemistry in an arid environment: a case study from northwestern Saudi Arabia. *Environmental Monitoring and Assessment*, 187, 1-18.

Zhang, X., Ma, Z., & Lu, H. (2018). Analysis of the hydro-chemical characteristics and origin of the karst groundwater, East Jinan city. In *IOP Conference Series: Earth and Environmental Science* (Vol. 189, No. 3, p. 032061). IOP Publishing.).